DEUTSCHES ELEKTRONEN – SYNCHROTRON

DESY 93-072
ZU-TH 12/93
June 1993

Relativistic Corrections to Photoproduction of J/ψ

H. Jung, D. Krücker

III. Physikalisches Institut, Lehrstuhl B, RWTH Aachen

C. Greub, D. Wyler

Institut für Theoretische Physik, Universität Zürich, Switzerland

ISSN 0418-9833

NOTKESTRASSE 85 · D-2000 HAMBURG 52

To be sure that your preprints are promptly included in the HIGH ENERGY PHYSICS INDEX, send them to (if possible by air mail):

DESY
Bibliothek
Notkestraße 85
W-2000 Hamburg 52
Germany

DESY-IfH
Bibliothek
Platanenallee 6
O-1615 Zeuthen
Germany

DESY 93-072
ZU-TH 12/93

June 11, 1993
ISSN 0418-9833

Relativistic corrections to Photoproduction of J/ψ

H. Jung and D. Krücker [1]

III. Phys. Institut, Lehrstuhl B, RWTH Aachen, FRG

and

C. Greub and D. Wyler [2]

Institut für Theoretische Physik, Universität Zürich, Switzerland

Abstract

We consider various models for photoproduction of J/ψ on protons, based on the well-known photon-gluon fusion mechanism. We show that relativistic corrections to the J/ψ bound state lead to a better description of the EMC and NMC data, especially in the high z region ($z > 0.8$) where the naive (nonrelativistic) colour singlet model breaks down (z is $E_{J/\psi}/E_\gamma$ in the proton rest frame). As most of the events are expected in this domain, these corrections are important for extracting the gluon distribution function from the data. We also discuss diffractive J/ψ production and a heuristic model for elastic production.

[1] supported by DFG
[2] partially supported by Schweizerischer Nationalfonds

1 Introduction

If the main contribution to J/ψ photoproduction can be attributed to the photon-gluon fusion mechanism, this process can be used to determine the gluon density inside the proton quite accurately. However, this requires a detailed understanding of the contribution of photon-gluon fusion to the J/ψ photoproduction cross section, including estimates of the various corrections. Higher order QCD effects, similar to those needed in open charm production, are usually parametrized by an overall factor (K factor). Up to now, K factors of $2-5$ were used to describe the measured inelastic J/ψ production cross section [1, 2, 3, 4, 5] within the model of photon-gluon fusion. Even when including such overall K factors, there is still a discrepancy between theory and data in the differential spectra. However, since we consider production of a bound state, one must also investigate relativistic corrections (i.e. (v/c)-effects) to the $c\bar{c}$ state produced; these can change the shape.

With the start of the high energy ep collider HERA, higher $\gamma\, p$ center-of-mass energies can be reached and new J/ψ production mechanisms could show up: In addition to elastic, target diffractive (where the final hadronic state on the proton side has relatively small mass) and inelastic J/ψ photoproduction, there could also be diffraction at the gamma vertex associated with a hard inelastic subprocess.

In this paper we give a detailed description of inelastic J/ψ photoproduction, emphasizing relativistic corrections to the bound state. We show that including these corrections the data available from present fixed target experiments [3, 4, 5] can be described quite well over the full phase space. These relativistic corrections yield a value for the charm quark mass m_c which agrees rather well with that calculated from potential models in the J/ψ decay [6].

We also discuss diffractive J/ψ production and argue that diffraction at the proton vertex is already included in our model for inelastic J/ψ production; no additional model is required here. On the other hand, a model based on the partonic picture of the Pomeron $\mathbb{P}$ [7] will be used to describe diffractive J/ψ production at the photon vertex. Then we also give estimates for elastic J/ψ production using a heuristic model based on a bound state picture of the Pomeron.

The outline of the paper is as follows: In section 2 we describe the four kinematical regions of interest. In section 3.1 we review the colour singlet model for inelastic J/ψ production and in 3.2 we include relativistic corrections, following a model of Keung and Muzinich [8]. Diffractive production is discussed in section 4 and in section 5 elastic J/ψ production based on the phenomenological Pomeron picture is sketched.

2 J/ψ production mechanisms

We consider J/ψ photoproduction

$$\gamma(q) + p(p_p) \to J/\psi(p_{J/\psi}) + X(p_X) \quad . \tag{1}$$

X denotes the hadronic final state and is simply a proton for the elastic process. Usually the variable z is introduced to describe the inelasticity of the process:

$$z = \frac{p_p \cdot p_{J/\psi}}{p_p \cdot p_\gamma} = \frac{E_{J/\psi}}{E_\gamma}\,|_{p\ rest\ frame} \quad . \tag{2}$$

For the elastic process z is mostly near 1, whereas for the inelastic process z is less than 1. The mass m_X distinguishes diffractive ($m_p \leq m_X \leq 3-5$ GeV) from inelastic ($m_X \geq 3-5$ GeV) processes.

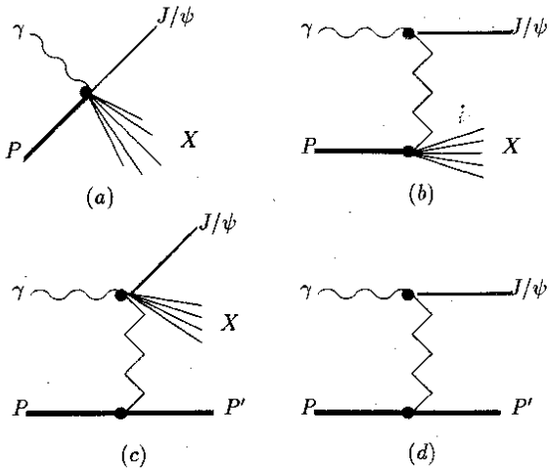

Figure 1: J/ψ production mechanisms: *a*. BI + TI, *b*. BE + TI, *c*. BI + TE, *d*. BE + TE. The zig-zag line represents any kind of momentum transfer.

In Fig. 1 we show diagrams for the different J/ψ production mechanisms. Following the somewhat arbitrary classification from low energy experiments ($\sqrt{s_{\gamma p}} \leq 20$GeV), one defines four different types of processes:

BI + TI: beam inelastic and target inelastic (Fig. 1a)

$$\gamma + p \to J/\psi + X \quad . \tag{3}$$

BE + TI: beam elastic and target inelastic (Fig. 1b)

$$\gamma + p \to J/\psi + X \tag{4}$$

BI + TE: beam inelastic and target elastic (Fig. 1c)

$$\gamma + p \to J/\psi + X + p \tag{5}$$

BE + TE: beam elastic and target elastic (Fig. 1d)

$$\gamma + p \to J/\psi + p \tag{6}$$

In all cases the hard subprocess can be described by photon-gluon fusion.

In photon-gluon fusion, a colour octet $c\bar{c}$ pair is produced. In order to obtain the correct colour and spin constraints of the J/ψ, one of the charm quarks emits a gluon in the final state

$$\gamma(q) + g_1(g_1) \to c(p_c) + \bar{c}(p_{\bar{c}}) + g_2(g_2) \quad . \tag{7}$$

At higher center of mass energies ($\sqrt{s_{\gamma p}} \geq 20$ GeV) other production processes like resolved photon and $B\bar{B}$ production with subsequent J/ψ decay are expected to show up. At $\sqrt{s_{\gamma p}} = 14.7$GeV the cross section for these processes are $\sim$ O(0.01nb) whereas for HERA energies we expect $\sim$ O(20nb). These processes will not be considered in this paper, because they can be easily suppressed by applying suitable cuts.

3 Inelastic J/ψ production

Inelastic J/ψ-production, Fig. 1a, is characterized by $z < 1$ and non-negligible $p_{\perp J/\psi}$. This process can be calculated in the QCD improved parton model since the scales involved are of the order of $m^2_{J/\psi}$.

3.1 Nonrelativistic colour singlet model

Photon-gluon fusion into a pair of charm quarks leads to a $c\bar{c}$ bound state, when the mass $m_{c\bar{c}} \leq 2m_{D^0}$, the lowest mass needed for open charm production.

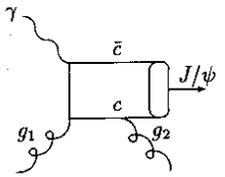

Figure 2: Feynman diagram for the subprocess $\gamma g \to J/\psi g$; the remaining 5 permutations are not shown.

In the so-called nonrelativistic colour singlet model [9] both charm quarks are at rest in the rest system of the J/ψ and $m_c = m_{J/\psi}/2$. Because of the emission of the gluon g_2 (see Fig. 2), the $c\bar{c}$ state has automatically spin 1. The 3 helicities of the J/ψ final state are represented by the matrices

$$A\mathcal{P}_i \quad , \mathcal{P}_i = \frac{1}{\sqrt{2}} \not{a}_i \frac{\not{p}_{J/\psi} + m_{J/\psi}}{2} \quad ; i = 0, +, - \quad , \tag{8}$$

where a^μ is the polarization vector of J/ψ and A is a normalization constant. The connection to the usual wave function description is given by

$$A = \sqrt{\frac{2}{m_{J/\psi}}}\psi(0) \quad . \tag{9}$$

These matrices $\mathcal{P}_i$ can be obtained by taking the well-known combinations of on shell quark and antiquark spinors appropriate to vector particles, e.g.,

$$\mathcal{P}_+ = v(\uparrow)\,\bar{u}(\uparrow) \quad . \tag{10}$$

In the following we use relation (9) and write all the results in terms of $\psi(0)$. To stay as model-independent as possible we extract this quantity from the measured leptonic decay width $\Gamma(J/\psi \to \ell^+\ell^-) = 5.4$ keV [10], using the QCD-corrected formula [11]:

$$\Gamma_{\ell\bar{\ell}} = \Gamma^0_{\ell\bar{\ell}}\,(1 - \frac{16}{3}\frac{\alpha_s}{\pi}), \tag{11}$$

where the lowest order width $\Gamma^{(0)}_{\ell\bar{\ell}}$ is given by

$$\Gamma^{(0)}_{\ell\bar{\ell}} = 16\pi e_q^2 \alpha_{em}^2 \frac{|\psi(0)|^2}{m^2_{J/\psi}}. \tag{12}$$

From the diagram in Fig. 2 and its permutations it is straightforward to write down the matrix element M for photon-gluon fusion. The contribution of the diagram explicitly shown in Fig. 2 reads:

$$M_1 = \mathrm{Tr}\left(\mathcal{P}\ \not{a}(g_2)\frac{\not{p}_c + \not{g}_2 + m_c}{2p_c g_2}\ \not{a}(g_1)\frac{\not{g}_1 - \not{p}_{\bar{c}} + m_c}{-2p_{\bar{c}}q}\ \not{a}(q)\right)\sqrt{\frac{2}{m_{J/\psi}}}\,\psi(0)\,g_s^2\,e\,e_q \quad . \tag{13}$$

Here $a(g_2)$, $a(g_1)$ and $a(q)$ denote the polarization vectors of the gluons and the photon, respectively.

For the differential cross section of the subprocess $\gamma\, g \to J/\psi\, g$ one gets

$$\frac{d\hat{\sigma}}{d\hat{t}} = \frac{1}{16\pi\hat{s}^2}\,|M|^2_{\Sigma,av} \quad , \tag{14}$$

where the quantity $|M|^2_{\Sigma,av}$ denotes the matrix element squared, and we have summed and averaged over the spins and colours of the final and initial state particles, respectively. The Mandelstam variable $\hat{t} = (p_{J/\psi} - q)^2$ varies in the interval $(m^2_{J/\psi} - \hat{s}, 0)$, where $\hat{s}$ is the center of mass energy of the incoming gluon and the photon. For $|M|^2_{\Sigma,av}$ one has

$$|M|^2_{\Sigma,av} = N\,\frac{\hat{s}^2(\hat{s} - m^2_{J/\psi})^2 + \hat{t}^2(\hat{t} - m^2_{J/\psi})^2 + \hat{u}^2(\hat{u} - m^2_{J/\psi})^2}{(\hat{s} - m^2_{J/\psi})^2(\hat{t} - m^2_{J/\psi})^2(\hat{u} - m^2_{J/\psi})^2}, \tag{15}$$

with

$$N = \frac{32}{3}(4\pi\alpha_s)^2\,(4\pi\alpha_{em})\,e_q^2\,m_{J/\psi}\,|\psi(0)|^2 \quad . \tag{16}$$

Here, $\hat{u}$ is fixed by the relation $\hat{s} + \hat{t} + \hat{u} = m^2_{J/\psi}$. Note that if one of the gluons has zero momentum, the above expression remains finite.

In order to get the γp cross section we convolute the partonic one in eq. (14) with the gluon distribution in the proton for which we use for simplicity the scaling function $xG(x) = 3(1-x)^5$.

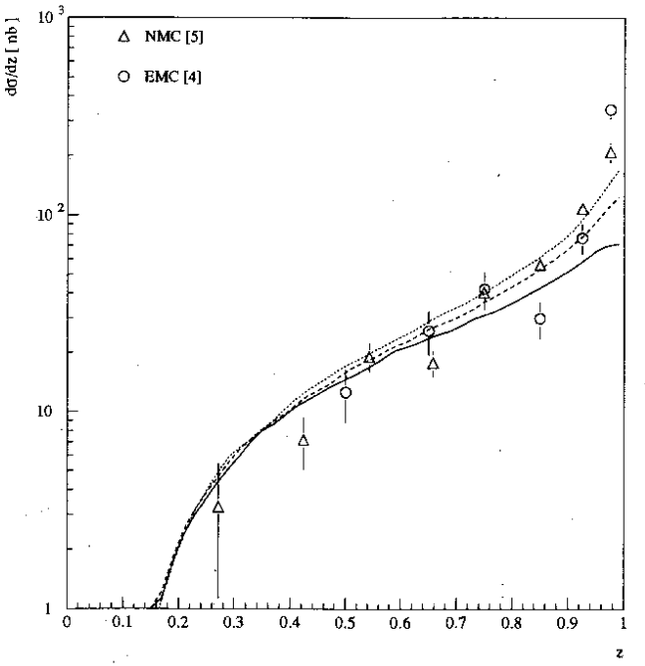

Figure 3: $d\sigma/dz$ without and with relativistic corrections. The distributions for different values for ϵ/m_c are shown ($\epsilon/m_c = 0$ solid line, $\epsilon/m_c = 0.16$ dashed line, $\epsilon/m_c = 0.3$ dotted line). A K-factor of $K = 2.0$ has been used. Also shown are the data from EMC,NMC [4, 5].

For the center of mass energies we consider, other choices of $xG(x)$ do not change the result significantly. The γp cross section then reads:

$$\frac{d^2\sigma}{dx\,dt} = G(x)\frac{d\hat{\sigma}}{d\hat{t}} \tag{17}$$

On the right hand side of eq. (17) $\hat{t}$ and $\hat{s}$ have to be replaced by t and $x \cdot s$, respectively. In Fig. 3 the solid line shows $d\sigma/dz$ calculated from the nonrelativistic colour singlet model for $\sqrt{s_{\gamma p}} = 14.7$GeV. Also the data of the EMC and NMC collaboration [4, 5] compiled for $\gamma\ p$ scattering [12] are given. We have omitted data from FTPS [1] and NA14 [2] since they use additional cuts for the event selection. In the numerical evaluations we took $\alpha_s = 0.3$. The K factor needed to describe the data of [4] for $z \leq 0.8$ is obtained by normalizing the prediction from the nonrelativistic colour singlet model (cs) in the range $0 \leq z \leq 0.8$ to the measured

cross section [4] in the same z range ($\sigma_{EMC}(z \leq 0.8) = 10.13$nb and $\sigma_{cs}(z \leq 0.8) = 4.98$nb). We get $K = 2.03 \simeq 2$ and we note that this value is different to the one quoted in [4] since we do not fit the z distribution. We note however, that even with an overall K factor the data in the high z region cannot be explained by this model. In the next section we show that relativistic corrections to the colour singlet model naturally improve the predictions in this region. For earlier attempts to explain the high z region, see [12, 13].

3.2 Relativistic Corrections to the Color-Singlet-Model

Since we are interested in the kinematical region near the edge of the phase space (z-region $z > 0.7$), the internal motion of the charm quarks inside the J/ψ might be important. Therefore we want to consider relativistic corrections which allow for $p_{\bar{c}} \neq p_c \neq 1/2 p_{J/\psi}$ and $m_c \neq 1/2 m_{J/\psi}$ and investigate their influence on the z distribution. The importance of the internal motion has been shown in [12] for the "open charm approach" where an improved description of the data in the high z region ($z \geq 0.8$) could be achieved. There, however, the normalization of the cross section was somewhat arbitrary.

The description of relativistic bound states in a confining theory is notoriously difficult and no satisfactory treatment exists up to now. There are both higher order QCD effects as well as kinematical corrections and several problems, such as gauge dependence, which must be dealt with. A simple model was investigated by Keung and Muzinich [8], where corrections due to the internal motion are included in leading order. More specifically, they write

$$p_c = 1/2 p_{J/\psi} + p$$

$$p_{\bar{c}} = 1/2 p_{J/\psi} - p$$

and in the J/ψ rest frame they set $p^0 = 0$, whereas $\vec{p}^{\,2}$ is fixed such that the charm quarks are on-shell. This fixes $\vec{p}^{\,2}$

$$\vec{p}^{\,2} = \frac{m_{J/\psi}^2}{4} - m_c^2 = m_c \epsilon + O(\epsilon^2) \quad . \tag{18}$$

In this equation, ϵ can be thought of as the binding energy defined by $m_{J/\psi} = 2 m_c + \epsilon$. (ϵ/m_c) is used as an expansion parameter and only linear terms are retained in the formulas.

As this model was originally discussed for the decay of J/ψ at rest [8], one might worry whether it can be adequately generalized to describe moving particles. Recently, a similar picture was considered for B-mesons [14]. Extending an idea of Altarelli et al. [15], the bound state model is defined there by the conditions

$$p_1^\mu + p_2^\mu = P^\mu \quad , \tag{19}$$

$$\sqrt{\vec{p_1}^{\,2} + m_1^2} + \sqrt{\vec{p_2}^{\,2} + m_2^2} = P^0 \quad , \tag{20}$$

where the P^μ is the four momentum of the bound state, made up of two constituents with masses m_1, m_2 and momenta p_1, p_2. Condition (20) in general implies, that at least one of the the masses m_1 and m_2 is momentum dependent. This simplified model yields fully covariant results, mainly as a consequence of (19) which was found to be necessary for full covariance.

Within this picture, the model of [8] is easily understood in the J/ψ rest frame as the case where $m_1 = m_2 = m_c$ with m_c considered to be fixed. In this case $\vec{p_1}^{\,2} = \vec{p_2}^{\,2}$ as given in eq. (18).

As shown in ref. [14], ϵ has an invariant meaning and thus the prescription of [8] is covariant. Technically, the covariantisation can be achieved by replacing the projector (eq. (2.11) in [8]) by:

$$\mathcal{P}_i = \frac{1}{\sqrt{2}} \frac{1}{\sqrt{E_c + m_c}\sqrt{E_{\bar{c}} + m_c}} \cdot (\not{p}_{\bar{c}} - m_c) \cdot \frac{\not{p}_{J/\psi} - m_{J/\psi}}{2 m_{J/\psi}} \cdot \not{a}_i \cdot \frac{\not{p}_{J/\psi} + m_{J/\psi}}{2 m_{J/\psi}} \cdot (\not{p}_c + m_c) \tag{21}$$

where p_c, and $p_{\bar{c}}$ are the momenta of the quark and antiquark (with $E_i = p_i^0$), respectively and $\not{a}$ refers to a massive vector particle with polarization a^μ. In the definition of $\mathcal{P}$ in eq. (21) we have included an extra factor $(1/\sqrt{2})$ with respect to eq. (2.11) in [8] in order to get the nonrelativistic $\mathcal{P}$ defined in eq. (8) in the limit $\epsilon \to 0$. The form (21) can be understood by boosting the naive rest frame ($p_{J/\psi} = (m_{J/\psi}, 0)$) spinor construction [14]. In the present context (eqs. (19) and (20)), this treatment is equivalent to the light-cone formalism [16] as shown in [14]. The correct normalization of the J/ψ bound state implies the integration measure

$$\sqrt{2 m_{J/\psi}} \frac{d^3 p}{(2\pi)^3} \frac{\psi(p)}{2\sqrt{m_c^2 + p^2}} \qquad p \equiv |\vec{p}| \quad . \tag{22}$$

Because the procedure is covariant, we obtain the corrected amplitude by writing the result in [8] covariantly. With the necessary crossing of the channels (Keung and Muzinich look at the decay of J/ψ particles) and keeping only order ϵ terms, the matrix element squared then reads:

$$\begin{aligned}
|M|^2_{\Sigma,av} \;=\; & N \left\{ \left(1 + \frac{5}{3}\frac{\epsilon}{m_c}\right) \frac{\hat{u}^2}{(m_{J/\psi}^2 - \hat{s})^2 (m_{J/\psi}^2 - \hat{t})^2} \right. \\
& - \frac{\epsilon}{12\, m_c} \Big[8 \left((m_{J/\psi}^2 - \hat{s})^4 + (m_{J/\psi}^2 - \hat{t})^4 \right) m_{J/\psi}^2 \\
& - 4 \left((m_{J/\psi}^2 - \hat{s})^3 + (m_{J/\psi}^2 - \hat{t})^3 \right) \left(10\, m_{J/\psi}^4 + 6 (m_{J/\psi}^2 - \hat{s})(m_{J/\psi}^2 - \hat{t}) \right) \\
& + \left((m_{J/\psi}^2 - \hat{s})^2 + (m_{J/\psi}^2 - \hat{t})^2 \right) \left(88\, m_{J/\psi}^4 + 82 (m_{J/\psi}^2 - \hat{s})(m_{J/\psi}^2 - \hat{t}) \right) m_{J/\psi}^2 \\
& - \left((m_{J/\psi}^2 - \hat{s}) + (m_{J/\psi}^2 - \hat{t}) \right) \left(88\, m_{J/\psi}^8 + 198 (m_{J/\psi}^2 - \hat{s})(m_{J/\psi}^2 - \hat{t})\, m_{J/\psi}^4 \right. \\
& \left. + 21 (m_{J/\psi}^2 - \hat{s})^2 (m_{J/\psi}^2 - \hat{t})^2 \right) \\
& + 32\, m_{J/\psi}^{10} + 228 (m_{J/\psi}^2 - \hat{s})(m_{J/\psi}^2 - \hat{t})\, m_{J/\psi}^6 + 126 (m_{J/\psi}^2 - \hat{s})^2 (m_{J/\psi}^2 - \hat{t})^2\, m_{J/\psi}^2 \Big] \\
& / \left((m_{J/\psi}^2 - \hat{s})^3 (m_{J/\psi}^2 - \hat{t})^3 (m_{J/\psi}^2 - \hat{u}) \right) \\
& \left. + \text{two cyclic permutations of } \hat{s},\, \hat{t} \text{ and } \hat{u} \right\}
\end{aligned} \tag{23}$$

The constant N is the same as in eq. (16) and in the limit $\epsilon \to 0$ expression (23) reduces to eq. (15).

In Fig. 3 we compare $d\sigma/dz$ calculated from the model including relativistic corrections (using the same K-factor as before) with the data of EMC[4] and NMC[5] for different values of ϵ/m_c. The result shows, that for $\epsilon > 0$ (where the model of [8] is defined), the large z region is enhanced giving a better representation of the data. In contrast, in the decay $J/\psi \to \gamma gg$ the region of high photon energies is depleted (as shown in Fig. 3 of [8]).

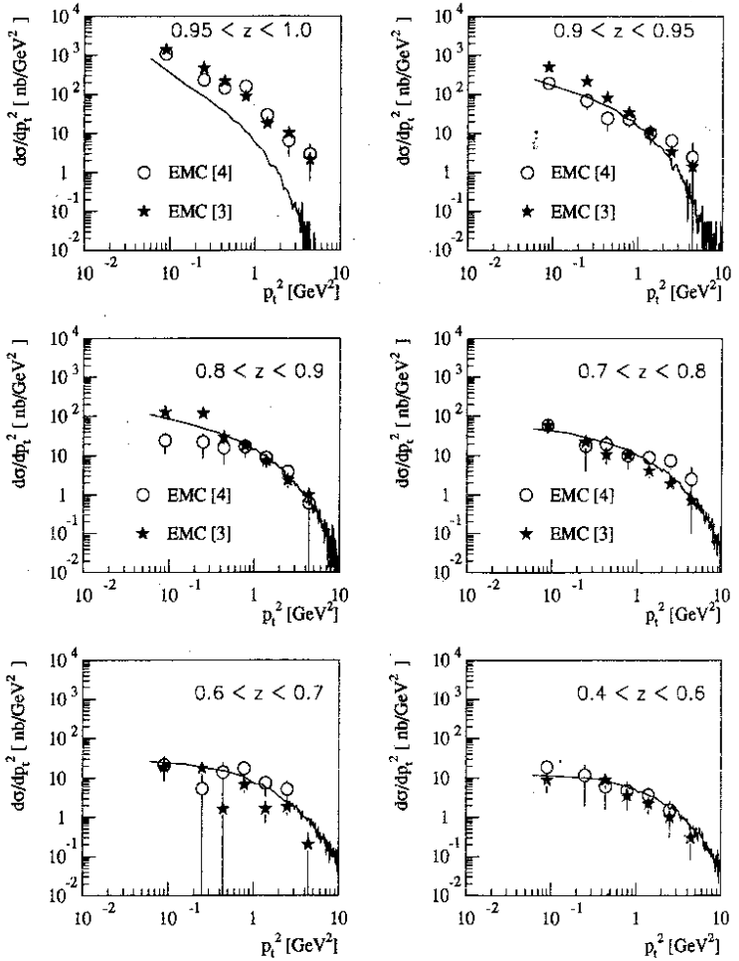

Figure 4: $d\sigma/dz/dp_\perp^2$ calculated from the model including relativistic corrections with $\epsilon/m_c = 0.16$ (histogram) (K=2.0) for different z-bins and compared to the data of [3, 4].

We can estimate ϵ/m_c from the ratio of gluonic and leptonic decay widths including radiative QCD corrections following the method of Mackenzie and Lepage [17]. There, $\Lambda_{\overline{MS}}$, as determined from the ratio Γ_{ggg}/Γ_{ll}, is different for J/ψ and Υ decays. But including relativistic corrections to the decays in question, ϵ/m_c can be fixed by requiring the two values of $\Lambda_{\overline{MS}}$ to coincide. Of course, an assumption about the relative size of ϵ/m in the c and the b system has to be made. Here we take ϵ to be constant, giving a smaller value of ϵ/m in the b system. Using the latest values of the decay widths [10] we obtain

$$\frac{\epsilon}{m_c} = 0.16 \tag{24}$$

and $\Lambda_{\overline{MS}} = 215$ MeV. The value for m_c is then given by

$$m_c = \frac{m_{J/\psi}}{2 + \epsilon/m_c} = 1.43\text{GeV} \quad . \tag{25}$$

This value agrees remarkably well with the numbers used in potential models for the J/ψ. We note that for the b system, $\epsilon/m_b \approx 0.05$. Again, the corresponding value for m_b lies within the expectations of the potential models. Also, it is reasonable that ϵ/m diminishes for bound states made of heavier quarks. This shows that (v/c) corrections, while probably not relevant in the Υ-system, are important in J/ψ physics.

One remark needed concerns the value of α_s we use. In the determination of ϵ/m_c from the ratio Γ_{ggg}/Γ_{ll}, $\alpha_s(\mu^2)$ is chosen in such a way that the first radiative QCD corrections vanish ($\alpha_s = 0.224$ with $\mu^2 = 0.44 \cdot m_{J/\psi}^2$) [17]. This special choice is adequate for the decay, but in the production of J/ψ the scale could be different. We use the standard value $\alpha_s = 0.3$ in all the calculations.

Using the value $\epsilon/m_c = 0.16$, we see from Fig. 3 that the data are described quite well even in the high z-region. In Fig. 4 we show the double differential cross section $\frac{d^2\sigma}{dp_\perp^2 dz}$ and compare the prediction with data. Here again, we see that the relativistic corrections move the theoretical prediction into the right direction to describe the data. However, in the highest z-region ($0.95 < z < 1.0$) also elastic J/ψ-production is expected, which then has to be added to the inelastic cross section. This will be discussed in section 5.2.

To conclude the chapter on inelastic J/ψ - photoproduction we have shown that it is possible to describe present data reasonably well using a simple model for relativistic corrections in bound states. This is an encouraging step towards understanding J/ψ photoproduction such that it can be used for a measurement of the gluon density inside the proton even in the high z - region, where most of the events are expected.

4 Diffractive J/ψ production

We call a process diffractive if the produced hadronic mass is restricted to the range $m_p < m_X < 3 - 5$ GeV. One distinguishes between the situation where the mass is produced "on the proton side" and on the beam side. Thus, both cases could be viewed as a particular case of the inelastic process. Nevertheless, the special situation may require an additional mechanism [13]. We would like to argue that the BE+TI case can be understood with the standard mechanism described in section 3, when including the relativistic corrections.

4.1 BE + TI

This process is characterized by a large value of z, usually $0.9 < z < 1$. We describe it in the same way as the purely inelastic production within the colour singlet model including relativistic corrections as described in the last section.

From Figs. 3 and 4 we see that the colour singlet model with relativistic corrections describes the data quite well down to $p_\perp^2 \simeq 0.1$ GeV^2 and up to $z \simeq 0.95$. In particular, the high z-region is enhanced. The agreement for $z > 0.95$ is not perfect, but probably the elastic contribution has to be included. This will be shown in chapter 5. Therefore, we do not expect a completely different production mechanism to account for the excess of events seen with $z > 0.95$, in contrast to [13].

4.2 BI + TE

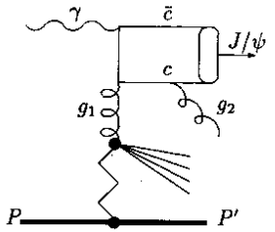

Figure 5: Diagram for the subprocess $\gamma p \to J/\psi + X + p$ via the subprocess $\gamma g_{I\!P} \to J/\psi g$.

Beam inelastic and target elastic J/ψ production (Fig. 5) is characterized by hadronic activity with low invariant mass m_X and the hadronic final state well separated in rapidity from the final state proton. In what follows we assume the proton to scatter elastically (i.e. stay a proton) but eventually diffractive dissociation of the proton could also take place still being separated in rapidity.

In our model we assume that the proton emits a Pomeron $I\!P$ which mainly consists of gluons [7, 18]. The $\gamma - I\!P - J/\psi$ vertex is described through the subprocess $\gamma + g_{I\!P} \to J/\psi + g_2$ where the gluon $g_{I\!P}$ now comes from the Pomeron. Since the Pomeron is by definition in a colour singlet state, a Pomeron remnant must appear which, together with gluon g_2 (from the hard subprocess), forms a colour singlet hadronic state. As there is no colour connection from this state to the final state proton, we expect a gap in the rapidity distribution. For the $p - I\!P - p$ vertex we use the ansatz of [19] but including a parameter $\hat{\epsilon}$ responsible for the rising total cross section seen in $p\bar{p}$ and recently in γp [20, 21] scattering experiments; $f_{p I\!P}(t, r)$ is the probability density that the proton (p) splits into a proton (p') and a Pomeron ($I\!P$) with momentum fraction r of the momentum of the incoming proton (p). This density depends on the momentum transfer $t = (p - p')^2$ and is

$$f_{p\,I\!P}(t,r) = \frac{\beta_{p I\!P}^2(t)}{16\pi} r^{1-2\alpha_{I\!P}(t)} \quad , \tag{26}$$

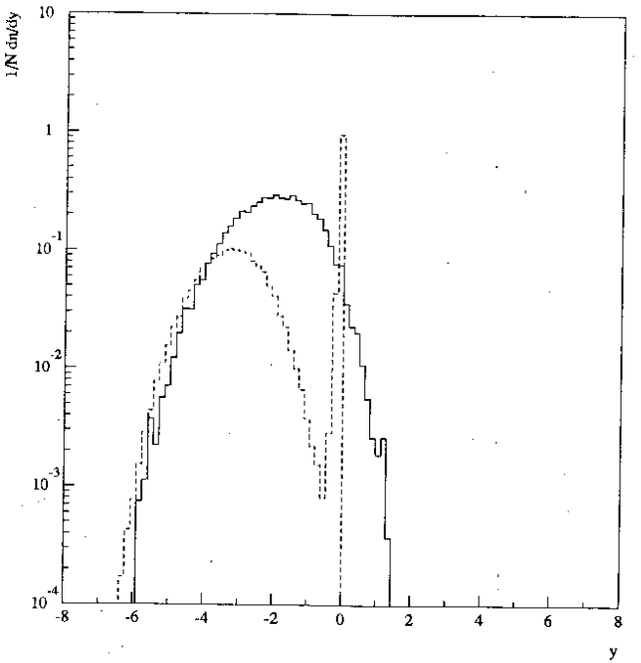

Figure 6: Rapidity distribution of the hadronic particles (except the J/ψ particle) for inelastic J/ψ production (BI+TI, solid line) and diffractive inelastic J/ψ production (BI+TE, dashed line). Note the elastically scattered proton has $\eta = 0$ and both distributions are normalized to the same number of events and not to the corresponding cross sections. A clear gap between the proton and the rest of the hadronic particles can be seen for the BI+TE process.

where

$$\beta_{p\,I\!P}(t) = \beta_{p\,I\!P}(0) e^{(-\frac{1}{2}R_N^2|t|)} \quad ; \quad \alpha_{I\!P}(t) = \alpha_{I\!P}(0) + \alpha'_{I\!P} t + \hat{\epsilon} \quad ;$$
$$R_N^2 = 3.3 GeV^{-2} \; ; \; \beta_{p\,I\!P}(0) = 10 \text{ GeV}^{-1} \; ; \; \alpha_{I\!P}(0) = 1 \; ; \; \alpha'_{I\!P} = 0.25 \text{ GeV}^{-2} \; ; \; \hat{\epsilon} = 0.085. \tag{27}$$

Since the gluon density in the Pomeron is not well known, two extreme choices are used in the literature [19]: $xG_0(x) = 6\ x\ (1-x)$ when the Pomeron consists of two gluons or $xG_5(x) = 6\ (1-x)^5$ when the gluon is as soft as in the proton. Recent data of UA8 [22] support a parton distribution of the form $xG_0(x)$.

The cross section for $\gamma + p \to J/\psi + X + p'$ as a function of the center of mass energy

squared (s) of incoming photon and proton reads now

$$\sigma(s) = \int f_{p\,\mathbb{P}}(t,r) \cdot G(x) \cdot \hat{\sigma}(\hat{s} = x\,r\,s)\, dr\, dx\, dt \quad . \tag{28}$$

Here $\hat{\sigma}(\hat{s})$ is the cross section for the hard subprocess $\gamma + g_{\mathbb{P}} \to J/\psi + g_2$ and it is obtained by integrating eq. (14) in the previous section over $\hat{t}$ in the range indicated there. The shape of the z distribution is the same as for purely inelastic production since in the p rest frame it only depends on $z = \frac{E_{J/\psi}}{E_\gamma}$. At EMC energies ($\sqrt{s} = 14.7$ GeV) we get (taking $K = 1$) $\sigma_{\gamma+p\to J/\psi+X+P} = 0.80(0.02)$ nb for $xG_0(x)$ and $xG_5(x)$ respectively, whereas for HERA energies ($\sqrt{s_{\gamma p}} \simeq 190$ GeV) we have $\sigma_{\gamma+p\to J/\psi+X+P} = 20.0(96.4)$ nb. In Fig. 6 we show the rapidity distribution of the final hadronic system and compare it with the prediction of the pure inelastic J/ψ photoproduction. One can clearly see the gap between the proton and the rest of the hadronic particles.

5 Elastic J/ψ production

In this section we want to estimate the rate for elastic J/ψ production within the physical pictures used above and present the result of a heuristic model where the proton emits a bound state of gluons ("Pomeron") which together with the photon produces a J/ψ.

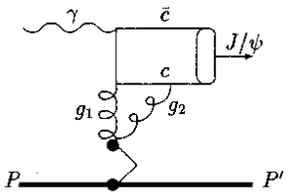

Figure 7: Pomeron model for elastic J/ψ production

A somewhat related model where the two gluons come directly from the proton was recently described by Ryskin [23]. Since this scheme is designed for off-shell photons, it is not directly applicable here.

5.1 Pomeron Model

In this picture (Fig. 7), valid at small t, the proton emits a Pomeron which is taken to be a bound state of two gluons. The emission of the Pomeron is described by eq.(26), while for the Pomeron bound state we make the ansatz

$$|\mathbb{P}> \;=\; \int \frac{d^2p_\perp\, dx\, \phi(p_\perp,x)}{16\,\pi^3\sqrt{x(1-x)}} \frac{1}{\sqrt{8}} \frac{1}{\sqrt{3}} \sum_c \left[\frac{1}{\sqrt{2}} \left(a^+_{c,\uparrow}(\underline{p_1})\, a^+_{c,\uparrow}(\underline{p_2})\right) + \right.$$
$$\left. + \frac{1}{\sqrt{2}} \left(a^+_{c,\downarrow}(\underline{p_1})\, a^+_{c,\downarrow}(\underline{p_2})\right) + \frac{1}{\sqrt{2}} \left(a^+_{c,\uparrow}(\underline{p_1})\, a^+_{c,\downarrow}(\underline{p_2}) + a^+_{c,\downarrow}(\underline{p_1})\, a^+_{c,\uparrow}(\underline{p_2})\right) \right] |0> \quad . \tag{29}$$

Here, $a^+_{c,r}(\underline{p_i})$ denotes a creation operator for a gluon with momentum $\underline{p_i}$, colour c and spin r. Eq. (29) postulates the Pomeron to be a linear combination of the three possible spin states for two gluons with equal weight. The momenta $\underline{p_i}$ are decomposed into transverse and light-front components according to the light-cone treatment [16]:

$$\underline{p_1} = (p_1^+, p_{1,\perp}) \quad , \quad \underline{p_2} = (p_2^+, p_{2,\perp}) \quad , \tag{30}$$

with

$$p_1^+ = x\,\mathbb{P}^+ \quad , \quad p_2^+ = (1-x)\,\mathbb{P}^+ \quad ,$$
$$p_{1,\perp} = x\,\mathbb{P}_\perp + p_\perp \quad , \quad p_{2,\perp} = (1-x)\,\mathbb{P}_\perp - p_\perp \quad . \tag{31}$$

In eq. (31), $p_\perp$ is the relative transverse momentum of the constituents. The state $|\mathbb{P}>$ is covariantly normalized to

$$< \mathbb{P}|\mathbb{P}' >= (2\,\pi)^3\, 2\,\mathbb{P}^+\, \delta^3(\underline{\mathbb{P}} - \underline{\mathbb{P}'}) \quad , \tag{32}$$

provided the wave function $\phi(p_\perp, x)$ satisfies

$$\int \frac{dx\, d^2p_\perp}{16\,\pi^3} |\phi(p_\perp,x)|^2 = 1 \quad . \tag{33}$$

In analogy to mesonic quark-antiquark bound states we will take a harmonic wave function

$$\phi(p_\perp, x) = C_a \exp\left(-\frac{p_\perp^2\, a^2}{x(1-x)}\right) \quad , \tag{34}$$

with an unknown parameter a. Eq. (33) implies $C_a = 8\,\pi\sqrt{3}$.

The parameter a can be related to the Pomeron radius $r_{\mathbb{P}}$ by defining the latter as the mean value of $b_\perp^2$ where $b_\perp$ is the Fourier conjugated variable of $p_\perp$. This yields

$$a = \frac{r_{\mathbb{P}}}{2\sqrt{3}} \quad . \tag{35}$$

In the numerical evaluations, we use the value $r_{\mathbb{P}} = 0.5$ GeV^{-1} [24].

This picture implies that the Pomeron is a particle which can decay into spin-one gluons. Of course spin can not be conserved since at $t = 0$, the Pomeron has spin one. The view that must be adopted here is that the expression is an analytic continuation of a physical state with even spin to the other points on the Pomeron trajectory. Clearly, the model itself as well as the definition of $r_{\mathbb{P}}$ are somewhat arbitrary, but we feel that it describes the physics appropriately.

The elastic rate can now be calculated in a straightforward manner. As the wave function is peaked at $p_\perp = 0$ and $x = 1/2$, i.e., the Pomeron emits two collinear gluons, both having half its longitudinal momentum, we evaluate the matrix element only at this configuration. For the differential cross section $d\sigma/dt$ we obtain:

$$\frac{d\sigma}{dt} = \frac{\pi}{m_{J/\psi}^2\, s} f_{p\,\mathbb{P}}(t, r = \frac{m_{J/\psi}^2}{s}) \overline{|M(\mathbb{P}\gamma \to J/\psi)|^2} \quad , \tag{36}$$

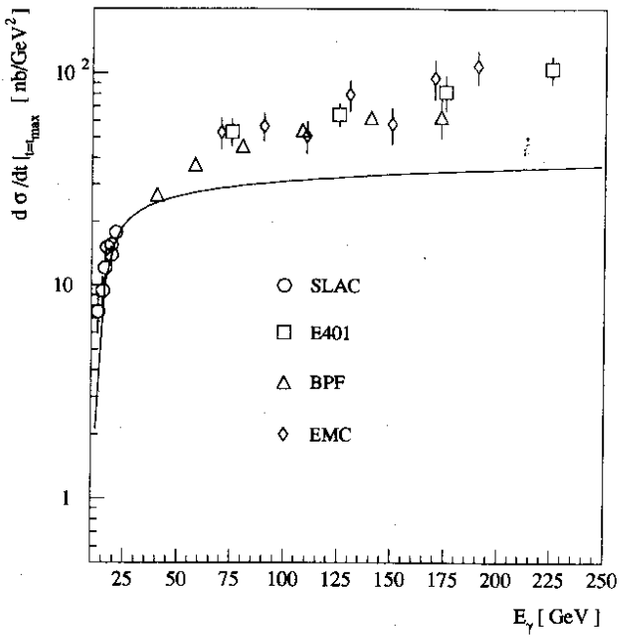

Figure 8: $d\sigma/dt|_{t=t_{max}}$ for elastic J/ψ photoproduction (including $K = 2.0$). The points are experimental data from SLAC, E401, BPF, EMC taken from [25].

with

$$\overline{|M(\mathbb{P}\gamma \to J/\psi)|^2} = \frac{8\,|\psi(0)|^2\,e_q^2\,(4\pi\alpha_s)^2\,(4\pi\alpha)}{9\,m_{J/\psi}^3}\left(1-\frac{11}{3}\,\frac{\epsilon}{m_c}\right)\left(\frac{9}{64\,r_{\mathbb{P}}^2}\right) \quad . \tag{37}$$

The last factor in eq.(37) represents the square of the integral

$$\int \frac{d^2p_\perp}{16\pi^3}\,\frac{dx\;\phi(p_\perp,x)}{\sqrt{x(1-x)}} = \frac{3}{8r_{\mathbb{P}}} \quad . \tag{38}$$

5.2 Comparison with Data

We compare the prediction of our model for elastic J/ψ production with data from different experiments [25]. In Fig. 8 we show $d\sigma/dt|_{t=t_{max}}$ as a function of the photon energy E_γ (in the rest frame of the proton). As before, we have included a K-factor $K = 2$. t_{max} is the maximal

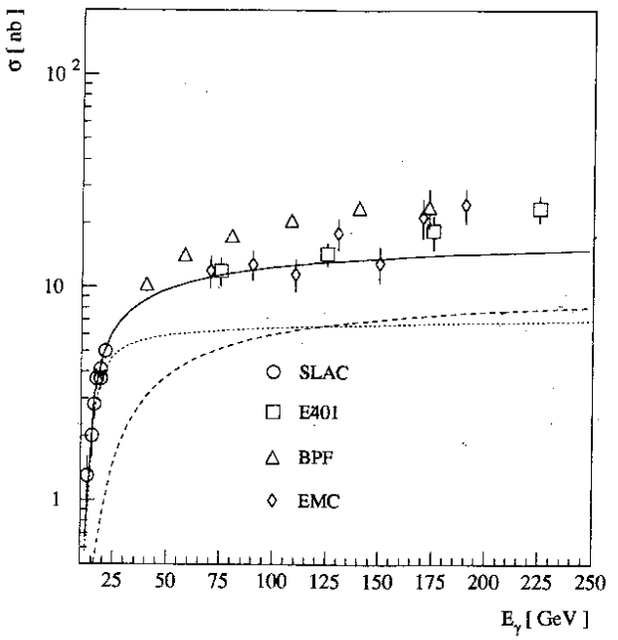

Figure 9: σ integrated over t for elastic J/ψ photoproduction (including $K = 2.0$). The elastic contribution is shown by the dotted line. The dashed line shows the inelastic contribution ($z > 0.95$) and the solid line is the sum. The points are experimental data from SLAC, E401, BPF, EMC taken from [25].

kinematically allowed value for t:

$$t_{max} = \frac{-(s-m_p^2)^2 + m_{J/\psi}^2\,(s+m_p^2) + (s-m_p^2)\sqrt{(s-m_{J/\psi}^2+m_p^2)^2 - 4sm_p^2}}{2s} \tag{39}$$

$$= 0 \text{ for } s \gg m_{J/\psi}, m_p \quad . \tag{40}$$

Whereas for $E_\gamma < 40$ GeV the theoretical curve is in good agreement with data, there is a marked discrepancy at higher energies. This disagreement can be partially explained by the experimental procedures. Elastic J/ψ production is not defined in all experiments in the same way: Some define an event to be elastic if $z > 0.95$. In others, the visible hadronic energy is cut, $E_{had} < 4.5$ GeV, in order to reject ψ' production. This implies in both cases that also

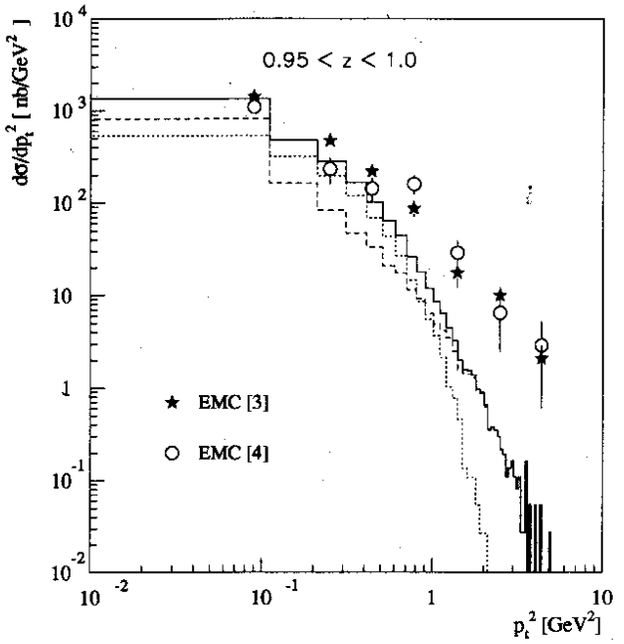

Figure 10: $d\sigma/dp_\perp^2$ for pure elastic (dotted) and inelastic (dashed) J/ψ photoproduction. The solid line is the sum of both contributions. The K - factor is 2. The data points are from [3, 4].

BI+TI contributes and hence a theoretical calculation based only on BE+TE is expected to lie below the data.

In Fig. 9 we show the t-integrated cross section for elastic J/ψ-production ($K = 2.0$) as a function of E_γ (for fixed target) and compare it again with data [25]. We now also show the prediction from inelastic J/ψ-production for $z > 0.95$. When adding the pure elastic (eq. (36)) and inelastic (eqs. (14,23)) ($z > 0.95$) contributions we see that the data are quite well described. We note that the main contribution for the rising of the cross section seen at large energies in Fig. 9 comes from the inelastic contribution and not from the pure elastic part, although we have included $\hat{\epsilon} = 0.085$ in the Pomeron parametrization.

In Fig. 10 we show the $p_\perp^2$ distribution for elastic and inelastic ($z > 0.95$) J/ψ-production and compare it with the data from EMC [3, 4] (see Fig. 4). We see that the data are well described at low $p_\perp^2$. In Fig. 11 the z distribution is shown for inelastic, elastic J/ψ photoproduction and the sum of both. Here it is obvious that in the data of EMC and NMC [4, 5] the highest z bin

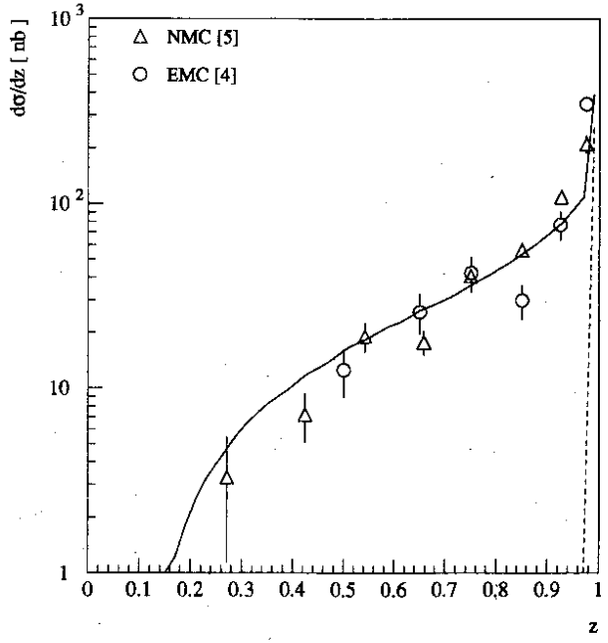

Figure 11: $d\sigma/dz$ for pure elastic (dashed) and inelastic J/ψ photoproduction. The sum of both contributions is shown with full line. The data points are from [4, 5].

includes the contribution from elastic J/ψ production. The presently available data are well described when adding the two contributions except for the highest z bin at large $p_\perp^2$.

6 Conclusions

In this paper we have investigated J/ψ photoproduction in various kinematical regions, taking the fundamental hard process to be photon-gluon fusion. In particular, we have emphasized the importance of relativistic corrections to the bound state (internal motion of the charmed quarks). These are especially important at the kinematical boundaries. In particular they enhance the high z-region, in agreement with the rise in the data.

We have then considered different models, depending on the kinematical regions. These include a Pomeron-based mechanism for the diffractive production and a simple gluon model

for the Pomeron in the elastic region. Combined with the relativistic corrections, the data are well described. We conclude, that photon-gluon fusion indeed accounts for photoproduction of J/ψ over a large range in z and $p_\perp^2$.

Our results for HERA are given in table 1. For HERA energies, there are several addi-

	BI + TI		BI + TE	BE + TE	resolved γ		$B\bar{B}$
	all	$z > 0.95$	G_0		$\chi \to J/\psi\gamma$	$J/\psi\gamma(g)$	
σ_0	23.3 nb	5.04 nb	20.0 nb	5.04 nb	13.0 nb	14.2 nb	0.54 nb
σ_1	76.4 nb	16.0 nb			15.6 nb	17.2 nb	1.2 nb

Table 1: Contributions to the photoproduction of J/ψ at HERA ($\sqrt{s} = 190$ GeV) without K factors. σ_0 denotes the cross sections when using the scaling function for $xG(x)$, whereas σ_1 gives the cross sections with the parametrization of [26], set B1, for $xG(x)$.

tional production mechanisms, such as "resolved photon" and $B\bar{B}$ production [12]. Their total contribution was estimated to be ~ 20 nb. They can be strongly suppressed by suitable cuts; for instance, a cut $z > 0.2$ reduces the resolved photon piece by a factor 10, which makes it negligible compared to the photon-gluon fusion process.

7 Acknowledgement

We are indebted to R. Eichler for raising our interest in diffractive J/ψ production and to S. Dangel and A. Salathé for collaboration at an early stage of the work. We are grateful to S. Baranov for many discussions on relativistic corrections. We would like to thank Z. Kunzst and P. Minkowski for helpful discussions.

References

[1] B.H. Denby et al., FTPS collaboration, *Phys. Rev. Lett.* 52, 795 (1984).

[2] R. Barate et al., NA-14 Collaboration, *Z. Phys.* C33, 505 (1987).

[3] J.J. Aubert et al., EMC Collaboration, *Nucl. Phys.* B213, 1 (1983).

[4] J. Ashman et al., EMC Collaboration, *Z. Phys.* C56, 21 (1992).

[5] M. de Jong, NMC Collaboration, *PhD Thesis* Utrecht (1991).
D. Allasia et al., NMC Collaboration, *Phys. Lett.* B258, 493 (1991).

[6] M. Baker, J.S. Ball and F. Zachariasen, *Phys. Rev.* D45, 910 (1992).

[7] G. Ingelman and P.E. Schlein, *Phys. Lett.* B152, 256 (1985).

[8] W.-Y. Keung and I.J. Muzinich, *Phys. Rev.* D27, 1518, (1983).

[9] E.L. Berger and D. Jones, *Phys. Rev.* D23, 1521 (1981).

[10] M. Aguilar-Benitez et al.,Particle Data Group, *Phys. Rev.* D45, (1992).

[11] R.Barbieri, R.Gatto, E.Remiddi, *Phys.Lett B* 106,497(1981)
W. Kwong, P.B. Mackenzie, R. Rosenfeld and J.L. Rosner *Phys. Rev.* D37, 3210 (1988).

[12] H. Jung, G.A. Schuler and J. Terron, *Int. J. Mod. Phys.* A32, 7955 (1992). DESY preprint 92-028 (1992).

[13] G.A. Schuler and J. Terron, DESY preprint 92-017 (1992) and CERN TH 6403-92 (1992).

[14] C. Greub and D. Wyler, *Phys. Lett.* B295, 293 (1992).

[15] G. Altarelli et al., *Nucl. Phys.* B208, 365 (1982).

[16] S.J. Brodsky and G.P. Lepage, *Phys. Lett.* B87, 959 (1979).

[17] P.B. Mackenzie and G.P. Lepage, *Phys. Rev. Lett.* 47, 1244 (1981).

[18] E.L. Berger, J.C. Collins, D.E. Soper and G.Sterman, *Nucl. Phys.* B286, 704 (1987).

[19] K.H. Streng, in Proc. of the workshop physics at HERA, Hamburg 1987, Ed. R.D. Peccei; also CERN preprint *CERN-TH* 4949, 1988.

[20] T.Ahmed et al., H1 Collaboration, *Phys. Lett.* B299, 374 (1993).

[21] M. Derrick et al., ZEUS Collaboration, *Phys. Lett.* B293, 465 (1992).

[22] A. Brandt et al. (UA8 Collaboration), in Proc. of the Joint Int. Lepton Photon Symposium & Europhysics Conf. of High Energy Physics, Geneva 1991, Ed. S. Hegarty, K. Potter, E. Quercigh

[23] M.G. Ryskin, *Z. Phys.* C57, 89 (1993).

[24] G. Ingelman and K. Prytz, DESY preprint 92-177 (1992).

[25] S.D. Holmes, W. Lee and J.E. Wiss, *Ann.Rev.Nucl.Part.Sci.* 35, 397 (1985).

[26] J.G. Morfin and Wu-Ki Tung, *Z. Phys.* C52, 13 (1991).